World Academy of Science, Engineering and Technology
International Journal of Chemical and Molecular Engineering
Vol:9, No:7, 2015

Synthesis and Properties of Chitosan-Graft Polyacrylamide/Gelatin Superabsorbent Composites for Wastewater Purification

H. Ferfera-Harrar, N. Aiouaz, N. Dairi

***Abstract*—**Superabsorbent polymers received much attention and are used in many fields because of their superior characters to traditional absorbents, e.g., sponge and cotton. So, it is very important but challenging to prepare highly and fast-swelling superabsorbents. A reliable, efficient and low-cost technique for removing heavy metal ions from wastewater is the adsorption using bio-adsorbents obtained from biological materials, such as polysaccharides-based hydrogels superabsorbents.

In this study, novel multi-functional superabsorbent composites type semi-interpenetrating polymer networks (Semi-IPNs) were prepared via graft polymerization of acrylamide onto chitosan backbone in presence of gelatin, CTS-g-PAAm/Ge, using potassium persulfate and N,N'-methylene bisacrylamide as initiator and crosslinker, respectively. These hydrogels were also partially hydrolyzed to achieve superabsorbents with ampholytic properties and uppermost swelling capacity. The formation of the grafted network was evidenced by Fourier Transform Infrared Spectroscopy (ATR-FTIR) and Thermogravimetric Analysis (TGA). The porous structures were observed by Scanning Electron Microscope (SEM). From TGA analysis, it was concluded that the incorporation of the Ge in the CTS-g-PAAm network has marginally affected its thermal stability. The effect of gelatin content on the swelling capacities of these superabsorbent composites was examined in various media (distilled water, saline and pH-solutions). The water absorbency was enhanced by adding Ge in the network, where the optimum value was reached at 2 wt. % of Ge. Their hydrolysis has not only greatly optimized their absorption capacity but also improved the swelling kinetic.These materials have also showed reswelling ability. We believe that these super-absorbing materials would be very effective for the adsorption of harmful metal ions from wastewater.

***Keywords*—**Chitosan, gelatin, **s**uperabsorbent, water absorbency.

I. Introduction

SUPERABSORBENT POLYMERS (SAPs) or hydrogels have three-dimensional network structure. They are not only able to absorb large amounts of aqueous fluids in a relatively short time, but also the absorbed water is hardly removed even under some pressure. They can undergo a change in volume (swelling/shrinkage) owing to their environmental stimulants responsive, such as temperature, pH, and ionic strength. These gels are occasionally referred to as smart materials [1], [2]. The SAPs applications is increasingly growing in special fields such as in hygienic products, agriculture, horticulture, wastewater treatment, drug delivery, water blocking tapes, food packaging, wave absorbing and sensors materials [3]-[5].

Many efforts have been supplied to enhance SAPsmaterials properties such as swelling rate and ratio and gel strength to meet applications requirement. Several SAPs have been designed by introducing inorganic particles, natural polymer nanofibers or by forming a semi- and full interpenetrating polymer networks (IPN) [6]-[9].

Even though the most of superabsorbents are based on synthetic polymers, such as acrylic acid and acrylamide, their broader use is limited by their toxic character and poor biodegradability. For environmental protection issues, the development of natural polymer-based superabsorbents has drawn much attention owing to their exceptional properties, i.e. biocompatibility, biodegradability, renewability, and non-toxicity as well as their low-cost production. As well, there is a growing notice for the application of SAPs materials having a biological origin in the removal of dyes or heavy metal ions from wastewater, which would contribute to resolve the environmental pollution. Since the cost of these materials is much lower than the commercial adsorbents, like activated carbon or ion exchange resins, the bio-adsorbents might gain a particular interest [10], [11].

Recently, the synthesis of eco-friendly SAPs through graft copolymerization of vinyl monomers onto natural polymer backbones has drawn much interest [12]-[14]. Among them, chitosan (CTS), a deactivated derivative of chitin and a copolymer of N-acetyl-glucosamine and N-glucosamine units, is a well affirmed polysaccharide owing to its inherent properties and antimicrobial activities [15], [16]. The grafting and copolymerization method allows to modify an easily available natural polymer such as CTS with a conventional and widely used synthetic hydrogel like cross-linked poly (acrylamide) [17]. Also, the presence of a large number of OH and NH_2 groups in CTS it confers a potential adsorption of heavy metal and dyes due to its chelating ability. Thus, it is likely to develop efficient low-cost bio-sorbents for the heavy metals by combining the metal ions attraction capacity of both natural polysaccharides and synthetic polymer [18], [19].

Gelatin (Ge) is a denatured derivative of protein collagen that is largely used in biomedical applications. Gelatin has a polyelectrolyte behavior, in where $-NH_3^+$ and $-COO^-$ groups are equal at isoelectric point (IEP) but these charges alter with

H. Ferfera-Harrar is an Professor in Chemistry Faculty, Department of Macromolecular Chemistry, at the University of Sciences and Technology Houari Boumediene USTHB, B.P. 32 El-Alia, 16111 Algiers, Algeria (Corresponding Author: e-mail: harrarhafida@yahoo.fr).

N. Aiouaz and N. Dairi are graduate students in Chemistry Faculty, Department of Macromolecular Chemistry, at the University of Sciences and Technology Houari Boumediene USTHB, B.P. 32 El-Alia, 16111 Algiers, Algeria.

the pH media. In our previous studies [20], [21], gelatin from bovine skin (IEP about 5.05) was used as organo-modifier to prepare organoclays from natural montmorillonite (Na-MMT). The pH of gelatin solutions were adjusted just below IEP (Ge chains riche in NH_3^+ groups) or above IEP (Ge chains riche carboxylic COO- groups) to allow its intercalation into MMT layers via electrostatic interactions or hydrogen bonds with MMT hydroxyl groups, respectively.

Hence, this paper is aimed to synthesize superabsorbent composites type semi-IPNs, in where the gelatin is used as the trapped soluble biopolymer in grafted network chitosan-graft-polyacrylamide (CTS-g-PAAm). It is planned to elaborate superabsorbents materials with improved biodegradability as compared to PAAm hydrogel and having highly swelling and retention capacities to trap pollutants from wastewater. Accordingly, we first prepared a series of CTS-g-PAAm/Ge composites, and then we hydrolyzed the elaborated materials. Since the adsorption of contaminants depends upon the swelling properties in various media, we focused our study on the influence of Ge content and hydrolysis treatment on the swelling capacities of the composites in various aqueous media and compared to that of the network. Structure, thermal, antibacterial and deswelling properties were also studied.

II. Experimental Section

A. Materials

Chitosan (CTS) with 75% deacetylated, medium molecular weight, and viscosity 200-800 cps was purchased from Sigma-Aldrich. Gelatin (Ge) type B extracted from bovine skin and with isoelectric point (IEP)= 5.05 was purchased from Merck Darmstadt., Acrylamide (AAm), Potassium persulfate (KPS) and N,N'-methylenebisacrylamide (MBA) from Fluka were used as received. Doubly distilled water was used for hydrogels preparation and swelling studies.

B. Preparation of the Superabsorbent Composites

A series of CTS-g-PAAm/Ge superabsorbent composites was prepared at various Ge content via graft copolymerization and crosslinking in aqueous solution at 60°C. The weight ratios of CTS, KPS and MBA with respect to AAm were kept constant. In typical procedure: 1g of CTS was dissolved in 30 mL 1% (v/v) acetic acid solution in three-neck flask, equipped with a reflux condenser, a funnel, a nitrogen line and a magnetic stirrer. After being purged with nitrogen, the flask was placed in water bath preset at 60°C for 30 min. Then, 0.1g of KPS was added, and the resulting mixture was gently stirred for an additional 15 min to generate radicals. Following this, a required amount of Ge that was previously dissolved in water at 40°C, was added to aqueous mixed solution of AAm (5g) and MBA (0.05 g, 1 wt. %) then kept under stirring at room temperature for 30 min. Subsequently, the mixture was introduced into the funnel, degassed for 15 min, and then added to the flask. The solution was stirred vigorously for another 3 h under nitrogen flux. The resulting hydrogel was neutralized to pH 8 by adding 1N NaOH solution, washed repeatedly with water and then dewatered two times with an excess of methanol. Finally, the gel particles were filtered and dried in an oven at 70°C. The product was ground (particles size 40-60 mesh) and stored away from moisture and light.

The networks CTS-g-PAAm and PAAm (without CTS) were also prepared according to the same procedure.

The alkaline hydrolysis of dried samples of CTS-g-PAAm and its Ge composites was carried out at 95 °C for 2 h using 1N NaOH solution. The obtained product was neutralized to pH 8 by adding acetic acid solution, dewatered with methanol, and then dried in an oven.

C. Characterizations

ATR-FTIR spectra were performed on Bio-Rad (Inc., USA) spectrometer model FTS-162. All samples were analyzed in the solid state as small grains.

The surface morphology of hydrogels samples was observed via Scanning Electron Microscope (SEM) on JEOL, Inc., USA). All samples were fixed on copper stubs and coated with gold before SEM observation.

Thermal stabilities of these superabsorbents were investigated using TGA analysis. The measurements were performed on a Q500 analyzer, TA instruments, at a heating rate of 10ºC/min, under a nitrogen atmosphere.

D. Measurements of Swelling Properties and Reusability

Swelling properties of CTS-g-PAAm superabsorbent and its composites were gravimetrically studied at room temperature.

Swelling rate of samples was calculated by measuring the water absorbency, *Qt*, at time t using (1). In brief, a weighted sample was immersed in water, taken out at desired time intervals. The weight of the sample was measured against time after wiping off the excessive water by gently tapping the surface with a wet filter. For the purpose to determine equilibrium water absorbency, Qeq, 0.15 g of each sample was immersed in selected swelling medium (400 mL) and allowed to soak to reach swelling equilibrium. The swollen sample was filtered through an 80-mesh stainless steel screen and drained for 30 min until no free water remained. *Qeq* value was calculated using (2).

$$Qt = (Wt - W0) / W0 \quad (1)$$

$$Qeq = (Weq - W0) / W0 \quad (2)$$

where, W0, Wt and Weq are the sample's weights in dry, swollen at time t and at equilibrium states, respectively. *Qt* and *Qeq* are calculated as grams of water per gram of sample.

The measurements of reusability were conducted for several times as follows: a sample of 0.10 g was immersed in 300 mL of distilled water until the swelling equilibrium was achieved. The swollen hydrogel was dried in an oven at 100°C. The water absorbency of samples after several times of reswelling was obtained according to (2).

III. Results and Discussion

A. Structural Analysis by ATR-FTIR

The chemical structures of the raw materials, the prepared

CTS-g-PAAm superabsorbent and its composites were studied by ATR-FTIR spectroscopy (Fig. 1). The ATR-FTIR spectra of CTS, crosslinked PAAm and CTS-g-PAAm network are shown in Fig. 1 (a). As it can be seen, the CTS spectrum shows mainly a broad absorption band around 3389 cm^{-1} due to ν_{O-H} and ν_{N-H}, the bands at 1657, 1598, 1379, 1320 and 1080 cm^{-1} that are assigned to $\nu_{C=O}$ (amide I) of acetyl groups, δ_{N-H} of NH_2 and NHCO groups, δ_{O-H} of hydroxyl, δ_{CO-NH} (amide III) and skeletal ν_{C-O-C} in anhydroglucose units, respectively [22].

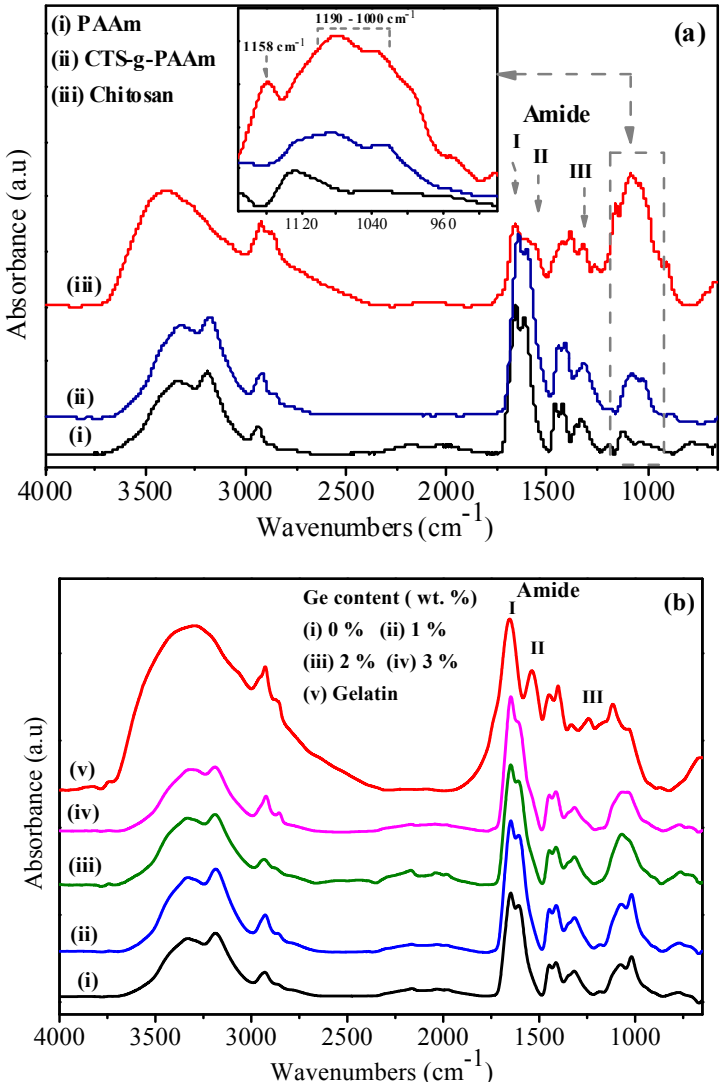

Fig. 1 ATR-FTIR spectra of (a) CTS, PAAm and CTS-g-PAAmsuperabsorbents and (b) gelatin and CTS-g-PAAm/Ge superabsorbent composites with different Ge contents

PAAm spectrum displays principally large bands at 3333 and 3186 cm^{-1} due to $\nu_{N-H\ (asym,\ sym)}$, respectively. The bands at 1645, 1600 and 1414 cm^{-1} are ascribed to $\nu_{C=O}$ (amide I), δ_{N-H} (amide II) and ν_{C-N} (amide III), respectively [23].

From CTS-g-PAAm spectrum, both components have mainly their bands in the same regions. Only an additional band near 1080 cm^{-1} characteristic of CTS, due to ν_{C-O-C} of piranose ring, is detected in a region non-disturbed by PAAm bands. This indicates that AAm was successfully grafted onto CTS backbone containing radical active sites, which were previously generated by the action of KPS as initiator.

Fig. 1 (b) regroups spectra of gelatin and CTS-g-PAAm/Ge superabsorbent composites. The Ge spectrum exhibits the bands of the amino acids mainly: amide A at 3315 cm^{-1} (ν_{N-H} coupled with hydrogen bonding), amide B at 2930 cm^{-1} (ν_{C-H}, ν_{N-H}), amide I at 1654 cm^{-1} (ν_{COO}, ν_{N-H}), amide II at 1540 cm^{-1} ($\delta_{N-H(sciss)}$,ν_{C-N}) and amide III at 1240 cm^{-1} (ν_{C-N}, δ_{N-H}). Besides, no additional bands or shoulders can be detected in composites spectra as compared to that of grafted network owing to the overlap of Ge bands with those of the network as well as to its relatively small amount, which does not exceed 3 wt. %.

In agreement with previous studies [17], [24], [25], the synthesis mechanism of CTS-g-PAAm/Ge composites is outlined in Fig. 2. The decomposition of persulfate ($S_2O_8^{2-}$) under heating generates sulfate anion-radicals (SO_4^{-}) that subsequently remove hydrogen from OH groups of CTS and

produce alkoxy radicals. These radicals initiate the AAm polymerization. The growth of PAAm chains onto CTS and crosslinking forms the CTS-g-PAAm network. Concurrently, Ge chains interpenetrated within this network and formed Semi-IPN superabsorbent composite.

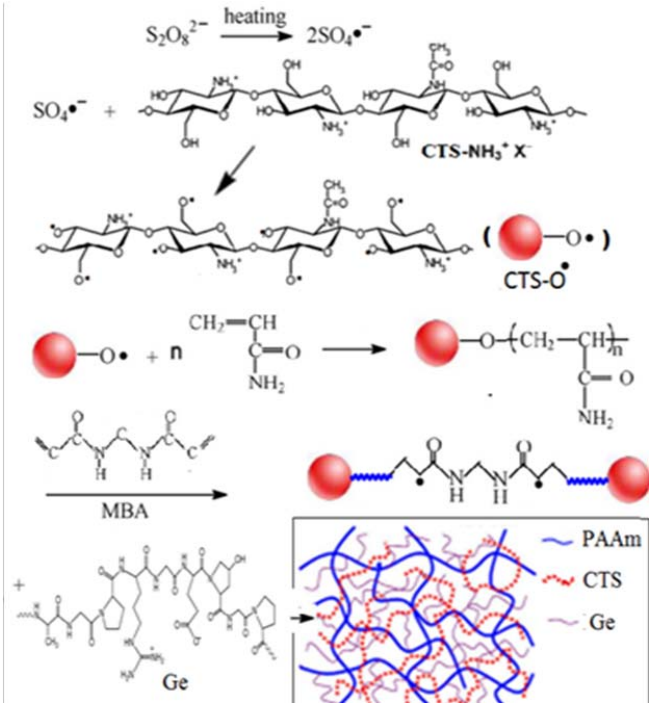

Fig. 2 Proposed mechanistic pathway for the synthesis of CTS-g-PAAm/Ge superabsorbent composites

The hydrolysis of the superabsorbents is also evidenced by ATR-FTIR analysis. The typical comparison of hydrolyzed PAAm and grafted network spectra, denoted H-PAAm and H-CTS-g-PAAm, with that of unhydrolyzed counterparts, is outlined in Fig. 3. It appears a new strong band at 1548 cm^{-1} due to asymmetric $\nu_{C=O}$ of carboxylate anions and another sharp peak at 1400 cm^{-1} due to their symmetric mode after the hydrolysis. In addition, the sharp decrease in the intensity band at 3185 cm^{-1}, due mainly to ν_{N-H} of amide groups, reveals that some of these groups were involved in the hydrolysis. During this treatment, the carboxamide groups of PAAm convert into carboxylate ions (COO^-) following by the release of ammonia. The hydrolyzed superabsorbent H-CTS-g-PAAm is therefore composed of $COONH_2$, COO^- and NH_2 groups, resulting in hydrogels with ampholytic properties.

The hydrolysis degree could be calculated by considering the absorbency ratio of both bands of carboxylate ions and amides groups [17]. The obtained values for the grafted network and its composites are in the narrow range 58-60 %, in agreement with PAAm-based hydrogels [26], [27].

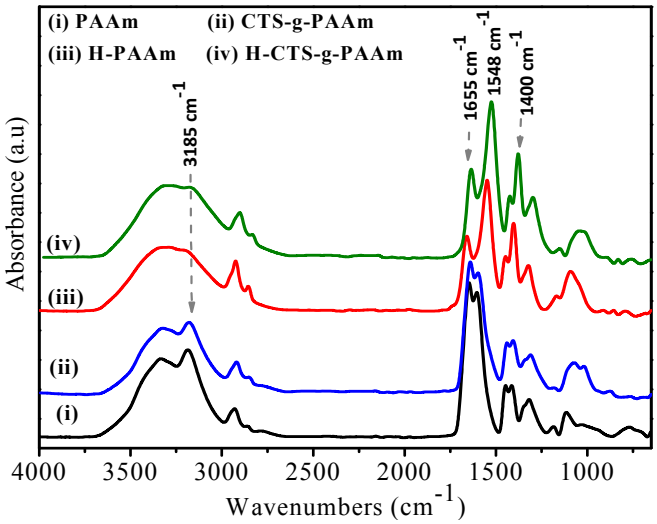

Fig. 3 ATR-FTIR spectra of the superabsorbents (i) PAAm, (ii) CTS-g-PAAm and their hydrolyzed counterparts (iii) and (iv), respectively

B. Morphological Study

As is well known, the surface porosity has great importance on swelling behavior of hydrogels. SEM micrographs of CTS, grafted network CTS-g-PAAm and typical composites containing 1 and 2 wt. % of Ge are shown in Fig. 4.

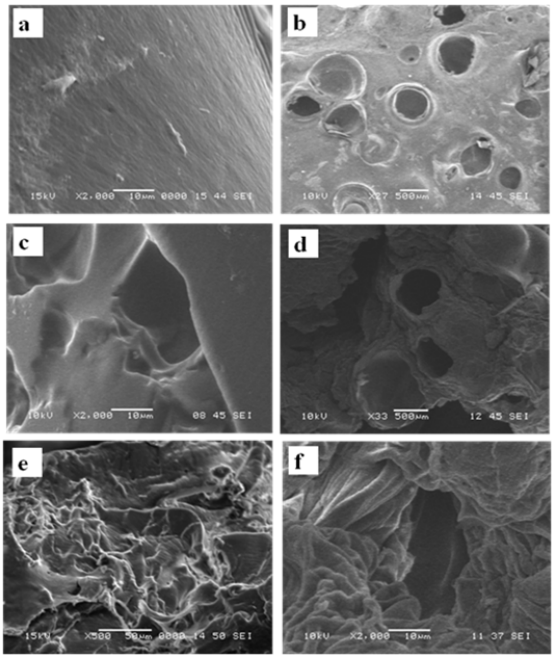

Fig. 4 SEM micrographs of (a) CTS, (b,c) CTS-g-PAAmand its composites containing Ge at (d) 1 and (e,f) 2 wt.%

CTS-g-PAAm network exhibits porous structure though no porosity is observed in CTS structure. It is supposed that these pores are convenient for the penetration of water and are the sites for the interaction of external stimuli with the hydrophilic groups of the network.

The surface of CTS-g-PAAm/Ge is visibly dissimilar from that of the grafted network. As can be seen, CTS-g-PAAm

displays a smooth and dense surface, whereas its gelatin composites exhibited rather loose and coarse surface in where some pores and gaps are observed. So, the incorporation of Ge chains improves the porous surface of the grafted network that is convenient to some extent for water uptake, suggesting the efficiency of the obtained network as an adsorbent of the pollutants in wastewater, which could move into the swollen network along with water through the porous structure.

C. Thermal Properties

Fig. 5 shows TGA and d(TG) thermograms of CTS, PAAm, CTS-g-PAAm networks and its composites. The formation of grafted CTS-g-PAAm can also be supported by TGA analysis, as shown in Fig. 5 (a). In CTS curves, besides the weight loss up to 120°C due to water, the thermal degradation of CTS occurs mainly in one step between 218 and 500°C due to random chains breaking and deacetylation [28]. The curves of PAAm exhibit three thermal decomposition steps. The first step occurs in the range of 150-220°C due to water loss adsorbed on the surface and in the pores of the network. The second step (220-298°C) is attributed to both weight losses of NH_2 of amide side groups in ammonia form and the cross-linker. The third one (298-440°C) is due to chain breakdown of PAAm. Besides, the grafted network containing 20 wt. % of CTS shows roughly similar thermal behavior as the PAAm hydrogel. The formation of CTS-g-PAAm grafted network via covalent linkages is confirmed by a significant improvement in its thermal stability compared to both components. The enhance in thermal resistance is evidenced by shifting of onset and maximum degradation temperatures (T_{onset},T_{max}) toward higher values as compared to PAAm and CTS. The values of T_{onset} and T_{max} of CTS-g-PAAm are an increase of about 30 and 28 °C for PAAm and 100 and 95 °C for CTS, respectively.

Besides, the effect of the addition of Ge on thermal stability of CTS-g-PAAm was also examined. TGA and d(TG) curves of Ge, CTS-g-PAAm network, and its composites are regrouped in Fig. 5 (b). The Ge curves display two thermal decomposition steps. The first step occurs up to 180°C due to moisture weight loss. The second one, in the range of 200-500°C, is attributed to the entire breakdown of protein chains, in where the T_{max} is reached at 311°C [29]. All composites display similar three steps degradation. The first step below 180°C is belonging to a loss of moisture and the second one in the range of 180-329°C is due to both amide groups and crosslinker losses. The third step above 330°C is due to substantial mass loss owing to chains breaking of compounds composites. Overall, the thermal resistance of composites is slightly improved, regardless Ge content, where T_{max} values are about 7 °C greater than that of CTS-g-PAAm.

D. Swelling Properties

1. Effect of Crosslinker

The diffusion of water and solute into hydrogels depends upon factors like crosslink density. So, preliminary syntheses of CTS-g-PAAm network were carried out by varying MBA weight ratio from 0.2 to 7 wt. %, while keeping the other reaction parameters constants. The effect of MBA amount on water absorbency in distilled water is shown in Fig. 6.

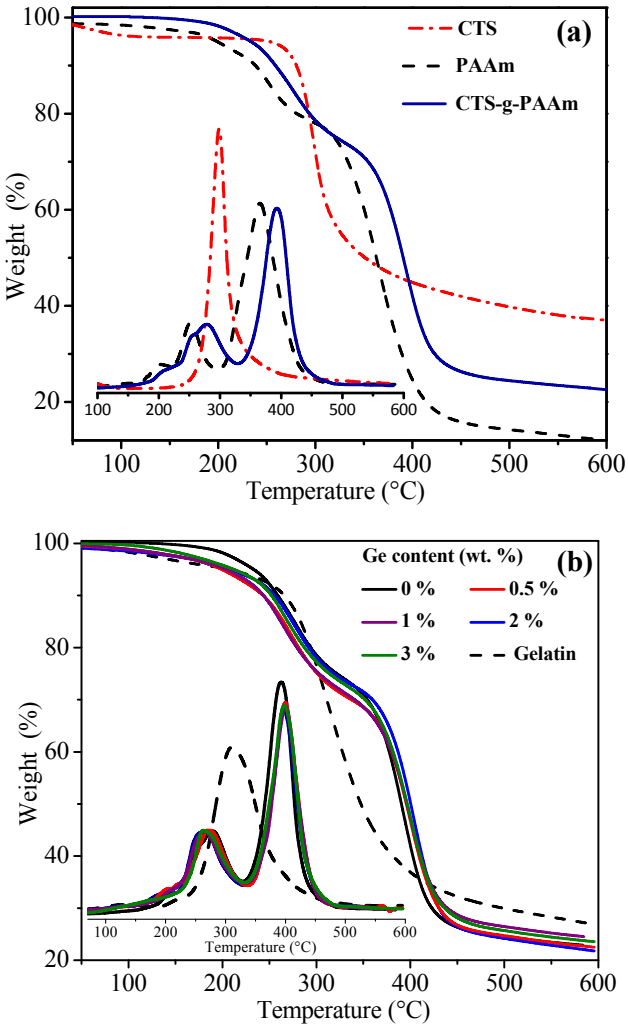

Fig. 5 (a), (b) TGA and d(TG) curves of CTS, PAAm, CTS-g-PAAm, Ge and CTS-g-PAAm/Ge superabsorbents composites

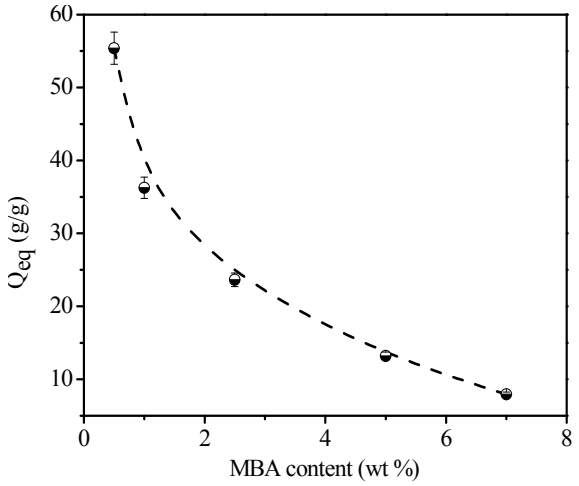

Fig. 6 Effect of Crosslinkercontent on water absorbency of CTS-g-PAAm hydrogel in distilled water

The water absorbency of hydrogel decreases as the content of MBA increases. As expected, the networks formed with a high content of MBA are strongly crosslinked, and the relaxation of PAAm chains is restricted, which in turn decreases the free spaces and thus smaller water diffuses inward matrix.For MBA< 0.18 wt. %, a slimy gel having a poor dimensional stability is formed, so that the swollen gel strength is not enough to be referred as a real superabsorbent. So, 1wt. % of MBA was selected in the synthesis of composites.

2. Effects of Ge Content and Hydrolysis

Fig. 7 displays the effect of Ge content on water absorbency of the CTS-g-PAAm superabsorbent and its composites in distilled water and 0.9 wt. % NaCl solution before and after hydrolysis. It is obvious from the curve in Fig. 7 (a) that when the amount of Ge in the feed mixture increases in the range 0.2-3 wt. % the equilibrium swelling ratios increases until 2 wt % of Ge, while beyond it a fall in absorbency is observed. Analogous behavior was reported for Semi-IPN hydrogel composed of sodium alginate-g-poly(sodium acrylate) (NaAlg-g-PNaA) network and linear polyvinylpyrrolidone (PVP) [30].

The results can be explained by the fact that increasing the proportion of hydrophilic Ge groups in the network increases the affinity for water thus resulting in a greater swelling ratio. This increase in swelling is also related to the polyelectrolytic behavior of Ge chains. Indeed, at IEP about 5.05 the amounts of NH_3^+ and COO^- groups are equal but changes when the pH media is higher or lower than IEP, as below:

$$NH_3^+—Ge—COOH \xleftarrow[pH<IEP]{H^+} NH_3^+—Ge—COO^- \xrightarrow[pH>IEP]{OH^-} NH_2—Ge—COO^- + H_2O$$

Therefore, in distilled water (pH 6~7), the electrostatic repulsion between the charges of same signs COO^- and $NH_3^+$of Ge chains causes their expansion, which promote the affinity of the network for water. Further than 2 wt. %, the density of Ge chains in the network increases and causes their entanglement. The elasticity of polymer chains in the network decreased and thus avoid that subsequent great water amount could be held.

Even though the similar trend of swilling in 0.9 wt. % NaCl solution is observed in Fig. 7 (b), the resultant values of water absorbency are less that in distilled water. This can be due to the osmotic pressure developed due to the difference in mobile ions concentration between the network and the aqueous solution. The optimal *Qeq* values for composite with 2 wt. % of Ge are about 62 $g.g^{-1}$in water and 51 $g.g^{-1}$in NaCl solution.

The curves in Figs. 7 (c) and (d) illustrate the swelling in distilled water and 0.9 wt. % NaCl solution, after hydrolysis of CTS-g-PAAm and its composites. Overall, the water absorbency of the hydrolyzed superabsorbents is remarkably higher than that of unhydrolyzed counterparts, while analogous swelling behavior is noticed before and after hydrolysis for both media. This significant increase in water absorption is obviously ascribed to the appearance of additional carboxylates COO^- on the grafted network host resulting from the hydrolysis of amide side groups of PAAm. The water absorbency of the unhydrolyzed superabsorbent composites containing 2 wt. % of Ge is only 62 $g.g^{-1}$, whereas that of hydrolyzed one reaches 570 $g.g^{-1}$. Also, it is noticed the extraordinary increase in water absorbency of all superabsorbents after hydrolysis. This behavior may arise from the contribution of another factor. For this purpose, the swelling capacities in distilled water of unhydrolyzed PAAm and CTS-g-PAAm superabsorbents are examined and compared to the hydrolyzed H-PAAm and H-CTS-g-PAAm counterparts. The water absorbency values obtained before hydrolysis are about 48 $g.g^{-1}$ forPAAm and 36 $g.g^{-1}$ for CTS-g-PAAm. Nevertheless, this order in swelling capacity is overturned for hydrolyzed counterparts, since the absorbency values became 180 g g^{-1} for H-PAAm and 382 $g.g^{-1}$ for H-CTS-g-PAAm. This result may be due to physical crosslinking involving CTS chains, which are promoted by a high temperature. Upon alkaline hydrolysis performed at 95 °C, specifics endothermic interactions such as type inter-chains hydrogen bonds can be formed between the groups of CTS chains (NH_2, OH) and underwent irreversible gelation process [31]. This unexpected formation of an additional physical gel further increases the swelling performance of the network. Similar swelling behavior was reported for superabsorbents chitin/carboxymethylcellulose [32].

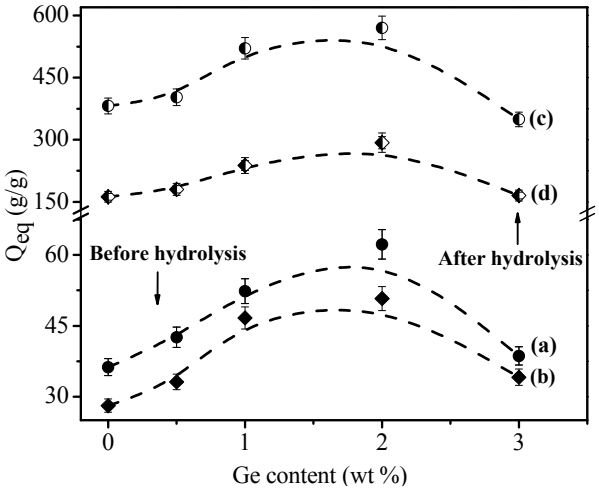

Fig.7 Variation of water absorbency of the superabsorbentsat different Ge content in (a), (c) distilled water and (b), (d) in 0.9 wt.% NaCl solution before and after hydrolysis, respectively

In the other hand, the undesired swelling-loss in 0.9 wt. % NaCl solution compared to distilled water, often observed in swelling of ionic hydrogels, is ascribed to the charge screening effect caused by Na^+ cations in the swelling medium, which shields the carboxylate anions and reduce the anion-anion electrostatic repulsions. The osmotic pressure between the network and the external solution decreases and the absorbed water is driven out of network [33].

Figs. 8 (a) and (b) show the effects of Ge content and hydrolysis on swelling rates of CTS-g-PAAm superabsorbent

and typical composites containing 1 and 2 wt. % of Ge in distilled water. Initially, the water absorbency increases fast with swelling time and then increases slowly until the swelling equilibrium is reached. Also, the swelling rates of hydrolyzed samples are higher than the unhydrolyzed counterparts. This speedy swelling of hydrolyzed materials is ascribed obviously to the added hydrophilic COO^- ions arising from hydrolysis. Additionally, during the hydrolysis the mixture becomes pasty, so the losses of NH_3 and water vapors create additional pores within the network. This porous structure promotes subsequent water diffusion through the network.

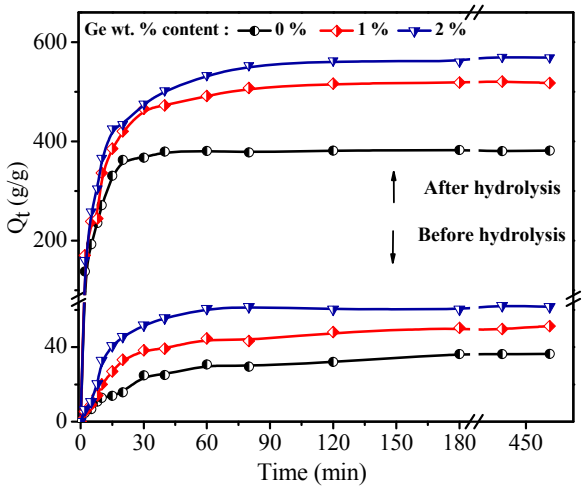

Fig. 8 Swelling rate for grafted CTS-g-PAAm superabsorbent and its composites with 1 and 2 wt. % of Ge, before and after hydrolysis

The pH-responsive swelling properties of superabsorbents were observed using buffer solutions with pH ranging from 2 to 12. Fig. 9 displays the pH-dependency on swelling of the unhydrolyzed CTS-g-PAAm and a typical composite having 2 wt. % of Ge together with their hydrolyzed counterparts. The swelling of both unhydrolyzed hydrogels are higher in the acid medium than in basic one with a maximum at pH~ 4. Since PAAm hydrogel is insensitive to pH owing to the absence of ionizable groups in its structure [34], this result is thus related mainly to the presence of CTS component, which is a weak base (pKa = 6.5). In the case of CTS-g-PAAm, the swelling in an acidic medium is controlled by the protonated amino groups of CTS. The electrostatic repulsions NH_3^+-NH_3^+ enhanced the osmotic pressure inside the network and the swelling of the hydrogel. In the basic region, the NH_3^+ ions of CTS change back to NH_2 groups and thus the swelling decrease.

For a composite, interacting species of Ge chains depending on the pH medium. At PHS $\leq$ 5 the swelling is promoted mainly by NH_3^+ species arising from both CTS and Ge chains, since carboxylic ions of Ge are protonated (COOH) [35].

At pH ~ 8-9, another maximum of low intensity is observed owing to the presence of COO^- groups of Ge that exert mutual electrostatic repulsions and cause an expansion of its chains, and hence a slight increase in swelling. This basic upmost swelling becomes more evident for both hydrolyzed superabsorbents due to the existence of COO^- ions resulting from hydrolysis. A similar observation has also been reported in studies on chitosan-based hydrogels [36], [37].

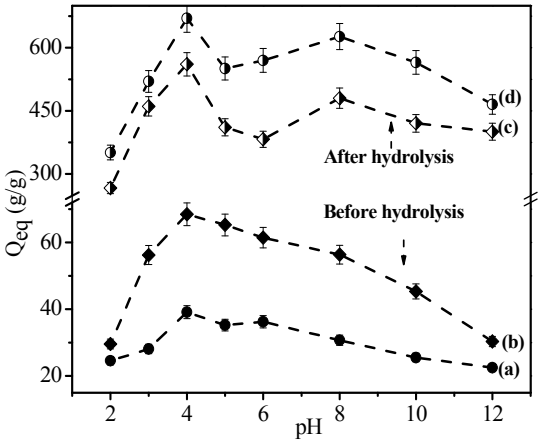

Fig. 9 pH-sensitivity of (a,c) CTS-g-PAAm and (b,d) itscomposite containing 2 wt. % of Ge, before and after hydrolysis

3. Reusability of Super Absorbents

Reswelling ability of a superabsorbent material is crucial for its practical applications and is related to the gel strength. Fig. 10 shows the effect of reswelling times on water absorbency in distilled water of typical samples of hydrolyzed superabsorbent CTS-g-PAAm and its composites prepared with 1 and 2 wt. % of Ge.The water absorbency of all the samples decreases gradually with increasing reswelling times. For the resulting dry H-CTS-g-PAAm, the water absorbency decreases from 382 to 228 g g^{-1} and about 60 % of its original water absorbency is kept after five times of reswelling. Likewise, composites samples still retain a high water absorbency of more than about 75 % of their original water absorbency. Like, the absorbency of hydrolyzed composite prepared with 2 wt. % of Ge is still as high as 426 g g^{-1}. This result indicates the effectiveness and reusability of these synthesized superabsorbents for technical applications, especially in wastewater purification.

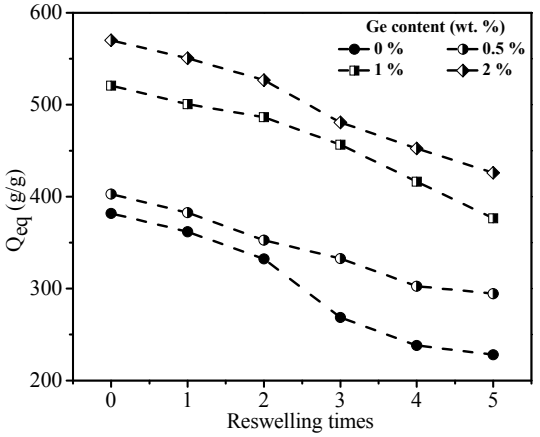

Fig. 10 Reswelling ability of the superabsorbents with different Ge content in distilled water

IV. Conclusions

Intelligent superabsorbent composites type s-IPNs were prepared via graft copolymerization of AAm onto CTS in the presence of gelatin at various contents. The grafted network has a porous structure and a more stable thermal degradation than its compounds. The incorporation of gelatin provided an increase in water uptake that decreased when the content of Ge was over than 2 wt. %.

Regardless Ge content, the water absorbency of CTS-g-PAAm/Ge composites is affected by pH changes and salinity. Besides, all hydrolyzed composites behaved as excellent super-absorbing materials and exhibited the highest pH and saline sensitivity. The reswelling experiments indicated the reuse of these superabsorbents.

This study will be extended to the application of these materials as bio-adsorbents systems in wastewater treatment.

References

[1] M.J.Zohuriaan-MehrKabiriK. Superabsorbent Polymer Materials: A Review. Iran Polym J (2008) 17:451-477.
[2] Buchholz F.L. Recent advances in super absorbent polyacrylates. Trends PolymSci (1994) 2:277-281.
[3] Kim J.Y., Kim T.H., Kim D.Y., Park N.G., Ahn K.D. Novel thixotropic gel electrolytes based on dicationicbis-imidazolium salts for quasi-solid-state dye-sensitized solar cells. J Power Sources, (2008) 175:692-697.
[4] Yang L., Yang Y., Chen Z., GuoC., Li S. Influence of super absorbent polymer on soil water retention, seed germination and plant survivals for rocky slopes eco-engineering, Ecological Eng (2014) 62:27–32.
[5] Zohuriaan-Mehr M.J., OmidianH., DoroudianiS., KabiriK. Advances in non-hygienic applications of superabsorbent hydrogel materials, J Mater Sci (2010) 45:5711–5735.
[6] KabiriK., OmidianH., Zohuriaan-Mehr M.J., DoroudianiS. Superabsorbent Hydrogel Composites and Nanocomposites: A Review, Polym. Composite (2011) 32:277-289.
[7] TangH., ChenH., DuanB., LuA., ZhangL. Swelling behaviors of superabsorbent chitin/carboxymethylcellulose hydrogels, J Mater Sci (2014) 49:2235–2242.
[8] ZhouY., FuS., ZhangL., ZhanH. Superabsorbent nanocomposite hydrogels made of carboxylated cellulose nanofibrils and CMC-g-p(AA-co-AM), CarbohydPolym (2013) 97:429–435.
[9] Dragan E.S. Design and applications of interpenetrating polymer network hydrogels: A review, ChemEng J (2014) 243:572–590.
[10] Wang L., Zhang J., Wang A. Fast removal of methylene blue from aqueous solution by adsorption onto chitosan-g-poly (acrylic acid)/attapulgite composite. Desalination (2011) 266:33–39.
[11] ZhangG., YiL., DengH., Sun P. Dyes adsorption using a synthetic carboxymethylcellulose-acrylic acid adsorbent. J. Environ Sci (2014) 26: 1203–1211.
[12] Chang C.Y., Duan B., CaiJ., Zhang L.N. Superabsorbent hydrogels based on cellulose for smart swelling and controllable delivery. EurPolym J (2010) 46:92-100.
[13] Lanthong P., Nuisin R., Kiatkamjornwong S. Graft copolymerization, characterization, and degradation of cassava starch-g-acrylamide/itaconic acid superabsorbents. Carbohydrate Polym (2006) 66:229-45.
[14] Pourjavadi A., Jahromi P.E., Seidi F., Salimi H. Synthesis and swelling behavior of acrylated starch-g-poly (acrylic acid) and acrylated starch-g-poly(acrylamide) hydrogels. Carbohydrate Polym (2010) 79:933-40.
[15] Mellegard H., Strand S.P., Christensen B.E., Granum P.E., Hardy S.P. Antibacterial activity of chemically defined chitosans: Influence of molecular weight, degree of acetylation and test organism. International J Food Microbiol (2011) 148:48-54.
[16] Muzzarelli R.A.A. Nanochitins and nanochitosans, paving the way to eco-friendly and energy-saving exploitation of marine resources. PolymSci: A Comprehensive Reference (2012) 10:153–164.
[17] Ferfera-HarrarH., AiouazN., Dairi N., Hadj-Hamou A.S. Preparation of chitosan-g-poly(acrylamide)/montmorillonite superabsorbent polymer composites: Studies on swelling, thermal, and antibacterial properties. J ApplPolymSci (2014) 131:39747.
[18] Shankar P., Gomathi T., Vijayalakshmi K., Sudha P.N. Comparative studies on the removal of heavy metals ions onto crosslinked chitosan-g-acrylonitrile copolymer, Inter J Bio Macromolecules (2014) 67:180–188.
[19] Maity J., Ray S.K. Enhanced adsorption of methyl violet and congo red by using semi and full IPN of polymethacrylic acid and chitosan, Carbohydrate Polym(2014) 104:8–16.
[20] Ferfera-Harrar H., Dairi N. Elaboration of cellulose acetate nanobiocomposites using acidified gelatin-montmorillonite as nanofiller: Morphology, properties, and biodegradation studies. Polym Composite (2013) 34:1515–1524.
[21] Ferfera-Harrar H., Dairi N. Green nanocomposite films based on cellulose acetate and biopolymer‐modified nanoclays: studies on morphology and properties. Iran Polym J (2014) 23:917-931.
[22] KumirskaJ., CzerwickaM., KaczyńskiZ., BychowskaA.,BrzozowskiK., ThömingJ., StepnowskiP. Application of spectroscopic methods for structural analysis of chitin and chitosan. Mar Drugs (2010) 8:1567-1636.
[23] Silverstein R.M., Bassler G.C, Morrill T.C. Spectrometric identification of organic compounds. (1991) John Wiley & Sons, New York.
[24] Pourjavadi A., AyyariM., Amini-Fazl, M.S. Taguchi optimized synthesis of collagen-g-poly(acrylic acid)/kaolin composite superabsorbent hydrogel. EurPolym J (2008) 44:1209- 1216.
[25] BaoY., MaJ., Li N. Synthesis and swelling behaviors of sodium carboxymethylcellulose-g-poly(AA-co-AM-co-AMPS)/MMT superabsorbent hydrogel. Carbohydrate Polym(2011) 84:76-82.
[26] Zhao Q., Sun J., Lin Y., Zhou Q. Superabsorbency, Study of the properties of hydrolyzed polyacrylamide hydrogels with various pore structures and rapid pH-sensitivities. Reactive FunctPolym (2010) 70:602-609.
[27] PourjavadiA., Mahdavinia G.R. Superabsorbency, pH-Sensitivity and Swelling Kinetics of Partially Hydrolyzed Chitosan-g-poly (Acrylamide) Hydrogels. Turkish JChem(2006) 30: 595-608.
[28] Zhou C., Wu Q. Novel polyacrylamide nanocomposite hydrogel reinforced with natural chitosan nanofibers. Colloid Surf B (2011) 84:155-162.
[29] Martucci J.F., Vázquez A., Ruseckaite R.A. Nanocomposites based on gelatin and montmorillonite morphological and thermal studies. J Therm Anal Calorim(2007) 89:117-122.
[30] Wang W., Wang A. Synthesis and swelling properties of pH-sensitive semi-IPN superabsorbent hydrogels based on sodium alginate-g-poly(sodium acrylate) and polyvinylpyrrolidone. Carbohydrate Polym (2010) 80:1028–1036.
[31] Chang C., Chen S., Zhang L. Novel hydrogels prepared via direct dissolution of chitin at low temperature: structure and biocompatibility. J Mater Chem (2011) 21:3865.
[32] Tang H., Chen H., Duan B., Lu A., Zhang L. Swelling behaviors of superabsorbent chitin/carboxymethylcellulose hydrogels. J. Mater Sci (2014) 49:2235–2242.
[33] Zhao Y., Kang J., Tan T. Salt-, pH- and temperature-responsive semi-interpenetrating polymer network hydrogel based on poly(aspartic acid) and poly(acrylic acid). Polymer (2006) 47:7702.
[34] Çaykara T., Doğmus M., Kantoğlu Ö. Network Structure and Swelling–Shrinking Behaviors of pH-Sensitive Poly(acrylamide-co-itaconic acid) Hydrogels. J PolymSci: Part B: PolymPhys (2004) 42:2586–2594.
[35] Bardajee G.R.,Pourjavadi A., Soleyman R. Novel highly swelling nanoporous hydrogel based on polysaccharide/protein hybrid backbone. J Polym Res (2011) 18:337–346.
[36] El-SayedM., Sorour M., Abd-El-Moneem N., Talaat H., Shalaan H., El-MarsafyN. Synthesis and properties of natural polymers-grafted-acrylamide. World ApplSci J (2011) 13:360-368.
[37] Mahdavinia G.R., Pourjavadi A., Hosseinzadeh H., Zohuriaan M.J. Modified chitosan 4. Superabsorbent hydrogels from poly(acrylic acid-co-acrylamide) grafted chitosan with salt- and pH-responsiveness properties.EurPolymJ(2004) 40:1399-1407.